Pathology International

Received: 30 October 2019 | Accepted: 9 January 2020

DOI: 10.1111/pin.12904

CASE REPORT

WILEY Pathology International

Distal-type bronchiolar adenoma of the lung expressing p16^{INK4a} – morphologic, immunohistochemical, ultrastructural and genomic analysis – report of a case and review of the literature

Mitsuhiro Tachibana[1] | **Masao Saito**[2] | **Jun Kobayashi**[2] | **Tadahiro Isono**[3] | **Yasushi Yatabe**[4] | **Yutaka Tsutsumi**[1,5]

[1] Department of Diagnostic Pathology, Shimada Municipal Hospital, Shizuoka, Japan

[2] Department of Thoracic Surgery, Shimada Municipal Hospital, Shizuoka, Japan

[3] Department of Surgery, Shimada Municipal Hospital, Shizuoka, Japan

[4] Department of Diagnostic Pathology, National Cancer Center Hospital, Tokyo, Japan

[5] Diagnostic Pathology Clinic, Pathos Tsutsumi, Aichi, Japan

Abbreviations:
ALK-1, anaplastic lymphoma kinase-1; BA, bronchiolar adenoma; *BRAF*, v-raf murine sarcoma viral oncogene homolog B1; CDX-2, caudal-type homeobox-2; CK, cytokeratin; CMPT, ciliated muconodular papillary tumor; EGFR, epidermal growth factor receptor; HPV, human papillomavirus; ISH, *in situ* hybridization; *KRAS*, *Kirsten RAS*; MUC, mucin; *NRAS*, *neuroblastoma RAS*; NSCLC, non-small cell lung carcinoma; OIS, oncogene-induced senescence; p16^{INK4a}, cyclin-dependent kinase inhibitor p16; TTF-1, thyroid transcription factor-1

Correspondence
Mitsuhiro Tachibana, MD, Department of Diagnostic Pathology, Shimada Municipal Hospital, 1200-5 Noda, Shimada, Shizuoka 427-8502, Japan.
Email: 0206mtachi@gmail.com

Bronchiolar adenoma (BA) of the lung is a rare benign neoplasm. Because of a chest abnormal shadow indicated by health checkup, a 77-year-old female nonsmoker underwent computed tomography, revealing an 8 mm ground glass nodule in the peripheral field of the right lower lobe. Wedge resection of the nodule was performed, with a frozen diagnosis of primary lung adenocarcinoma. The localized, 8 × 4 × 3 mm-sized, jelly-like mass microscopically revealed a lepidic-growing lesion composed of ciliated columnar cells, mucous cells and basal cells surrounded by mucin pool. Neither nuclear atypia nor mitotic activity was noted. Immunohistochemically, the ciliated, mucous and basal cells were positive for TTF-1 and p16^{INK4a}. Mucous cells were positive for napsin A and focally expressed MUC5AC. MUC6 was negative. Basal cells were positive for CK5/6, p40, p63 and podoplanin. Human papillomavirus genome was undetectable by *in situ* hybridization. Ultrastructurally, the bronchiolar epithelial tubules consisted of two layers, the inner nonciliated microvillous cells and the outer basal-like cells, and some of the inner cells were filled with mucin granules in cytoplasm. Molecular analysis of the tumor failed to show driver mutations. The final diagnosis was distal-type BA. The postoperative course was uneventful for 6 months.

KEYWORDS
bronchiolar adenoma, distal-type, electron microscopy, p16^{INK4a}, pulmonary benign tumor

INTRODUCTION

Bronchiolar adenoma (BA) of the lung is a newly recognized rare peripheral lung tumor histologically characterized by nodular proliferation of bilayered benign-looking bronchiolar-type epithelium with a continuous layer of basal cells. BA was first reported as ciliated muconodular papillary tumor (CMPT) in 2002 by Ishikawa.[1] The majority of the BA lesions, however, do not fit all of the diagnostic criteria of CMPT; BA often exhibits only focal or no papillary architecture, and contains variable numbers of ciliated and mucinous cells, with some lesions entirely lacking one or both of these components.[2,3] The morphologic and immunohistochemical features resemble proximal bronchioles (32%) or respiratory bronchioles (68%). The proximal-type is characterized by moderate to abundant mucinous and ciliated cells with negative or weak thyroid transcription factor-1 (TTF-1), while the distal-type reveals scanty or absent mucinous and ciliated cells with positivity of TTF-1.[2]

We report herein a surgical case of distal-type BA expressing cyclin-dependent kinase inhibitor p16 ($p16^{INK4a}$), with demonstration of ultrastructural features and review of the literature.

CLINICAL SUMMARY

A 77-year-old Japanese female nonsmoker was referred to Shimada Municipal Hospital because of a chest abnormal shadow on the chest X-ray in routine health checkup. Four years earlier, she had suffered from breast cancer without recurrence. Chest computed tomography revealed an 8 mm solitary ground glass nodule without cavitation or pleural retraction in the peripheral field of the right lower lobe of the lung, and the tumor was penetrated by a peripheral bronchiolo-arterial bundle (Fig. 1). No radiological and clinical features of interstitial lung disease were recognized. Neither lymphadenopathy nor metastatic lesions were noted. During the follow-up for 7 months, the lesion showed no size change. Primary lung cancer was suspected with a differential diagnosis of metastatic mammary carcinoma, and she was admitted for surgical intervention. The intraoperative frozen section diagnosis was adenocarcinoma, mimicking adenocarcinoma *in situ*, invasive mucinous adenocarcinoma or minimally invasive adenocarcinoma. Video-assisted thoracoscopic wedge resection of the lung tumor was performed. The patient did not receive adjuvant therapy, and is currently doing well, 6 months after surgery.

PATHOLOGICAL FINDINGS

Gross morphology

Grossly, the lesion displayed a localized, $8 \times 4 \times 3$ mm-sized and whitish tumor with gelatinous quality. No pleural retraction was observed. The resected margins were negative for tumor tissue.

Microscopic findings

The microscopically ill-defined nodular lesion showed a lepidic growth pattern, conforming to the preexisting pulmonary architecture (Fig. 2a). Bronchiolar epithelia grew with inflammatory stroma, and their cytoplasm contained gastric foveolar- or glandular-like mucin (Fig. 2b). Papillary architecture was unremarkable. Close microscopic observation demonstrated a bilayered pattern of growth: basal cells surrounded luminal columnar cells (Fig. 2c). Ciliated cells were focally identified (Fig. 2d). Elastic fiber staining demonstrated focal loss or disruption of alveolar elastic framework (Fig. 2e). The tumor cells lacked nuclear atypia and mitotic figures. The alveoli located at the periphery of the lesion were filled with alcianophilic mucin (Fig. 2f).

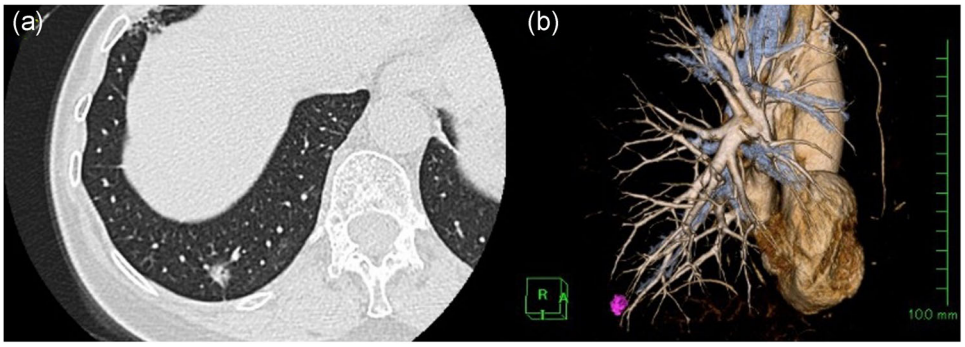

Figure 1 Clinical imaging. (**a**) A chest computed tomography image reveals an 8 mm solitary groundglassed nodule in the peripheral field of the right lower lung lobe. (**b**) The tumor, illustrated in purple color, is penetrated by a peripheral bronchiolo-arterial bundle.

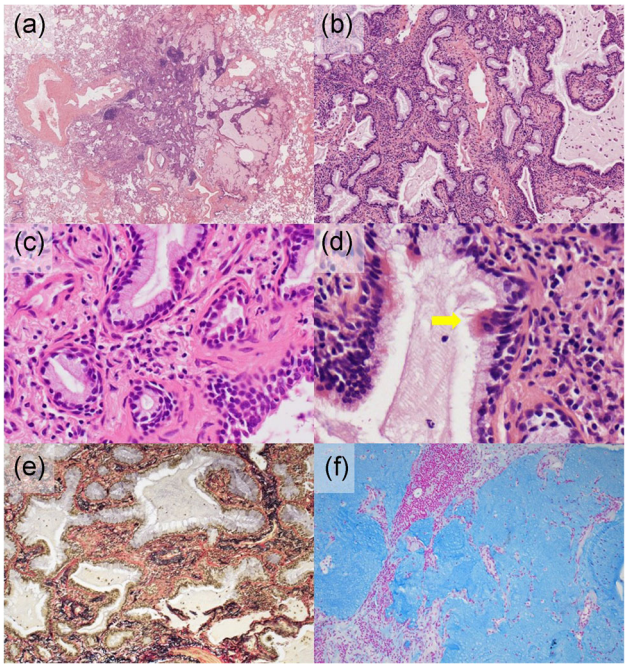

Figure 2 Microscopic findings of the lung tumor. (**a**) The lung parenchyma contains a defined nodular lesion with lepidic glandular growth and mucin secretion (HE). (**b**) Bronchiolar epithelia grow with inflammatory stroma, and gastric foveolar or glandular-like mucin is observed in the cytoplasm (HE). (**c**) High-powered view reveals a bilayered pattern of growth: basal cells surround the luminal columnar cells (HE). (**d**) A few ciliated cells are distributed (arrow) (HE). (**e**) Elastica van Gieson stain demonstrates focal loss or disruption of the alveolar elastic framework. (**f**) The alveoli at the periphery of the tumor are filled with alcianophilic mucin (Alcian blue, pH 2.5).

Immunohistochemistry

As indicated in Fig. 3, the ciliated, mucous and basal cells expressed cytokeratin 7 (CK7), thyroid transcription factor-1 (TTF-1: clone 8G7G3/1) and p16^{INK4a} (clone: G175-405). β-catenin revealed membranous and cytoplasmic staining. The ciliated columnar and mucous luminal-sided tumor cells were positive for napsin A, carcinoembryonic antigen and mucin 1 (MUC1). MUC5AC was focally expressed in the cytoplasm of the mucous cells. The basal cells were positive for CK5/6, p40, p63 and podoplanin (clone D2-40). Ki-67 labeling index was 3%. Negative markers included CK20, caudal-related homeobox protein-2 (CDX2), p53, chromogranin A, synaptophysin, MUC2, MUC6 and hepatocyte nuclear factor-4α. Anaplastic lymphoma kinase-1 (ALK-1) protein was negative (ALK iScore 0), employing the HISTOFINE ALK iAEP kit (Nichirei Bioscience, Tokyo, Japan). Programmed death-ligand 1 (clone: 22C3) was also negative.

Ultrastructural findings

The bronchiolar epithelial tubules consisted of two layers; the inner nonciliated microvillous cells and outer basal-like cells. Some (but not all) of the inner cells were filled with mucin granules in the cytoplasm. The cytoplasm of the basal cells was scanty. Ciliated cells were not included in the specimen evaluated. Representative fine structural features are demonstrated in Fig. 4.

Molecular findings

We evaluated gene mutations of v-raf murine sarcoma viral oncogene homolog B1 (*BRAF*V600E), *Kirsten RAS*, *neuroblastoma RAS* and epidermal growth factor receptor (EGFR: exons 18, 19, 20 and 21). In brief, real-time polymerase chain reaction (PCR) was applied to the detection of *BRAFV600E* mutations using a fluorescent oligonucleotide probe. PCR-reverse sequence specific oligonucleotide method was utilized for the *RAS* gene analysis. Mutation analysis of EGFR was performed with real-time PCR employing scorpion-amplification refractory mutation system. No mutations were demonstrated. Because of p16^{INK4a} expression, human papillomavirus (HPV) DNA was examined by *in situ* hybridization (ISH) assay employing biotinylated cocktail probes for both high and low risk HPV (Enzo Life Sciences, Farmingdale, NY, USA). HPV genome was not detected in tumor cell nuclei.

DISCUSSION

Bronchiolar adenoma is an extremely rare lung tumor.[2] Ishikawa[1] reported the first case in 2002, and named it ciliated muconodular papillary tumor. Literature review indicated a total of 68 cases reported to date.[1–10] The clinicopathological features of the previously reported cases are summarized in Table 1. The tumor size ranged from 2 to 15 mm. BA was often observed in middle-aged and elderly individuals (median age, 67 years), while a case of a 19-year-old girl was reported in the literature.[4] BA occurred in both men and women (M/F = 34:36), with no preference on the location in the lung. BA was histologically featured by bilayered growth of bronchiolar-type luminal columnar cells and basal cells (CK5/6, p40 and p63-positive) forming a continuous layer, recapitulating various levels of the bronchiolar tree. Based on morphologic and immunohistochemical features of the respective portions of the bronchiolar tree, Chang *et al.*[2] divided BA into proximal and distal types. The present lesion belonged to the distal-type BA. Neither recurrence nor distant metastasis has been reported during 1-month to 10-year follow-up periods after surgery.

Bronchiolar adenoma seems to be an indolent tumor with a very good prognosis, leading some investigators to question whether it is a reactive or hamartomatous lesion. However, the very recent molecular study of BA has identified *BRAF* V600E mutations (38%), unusual *EGFR* exon 19

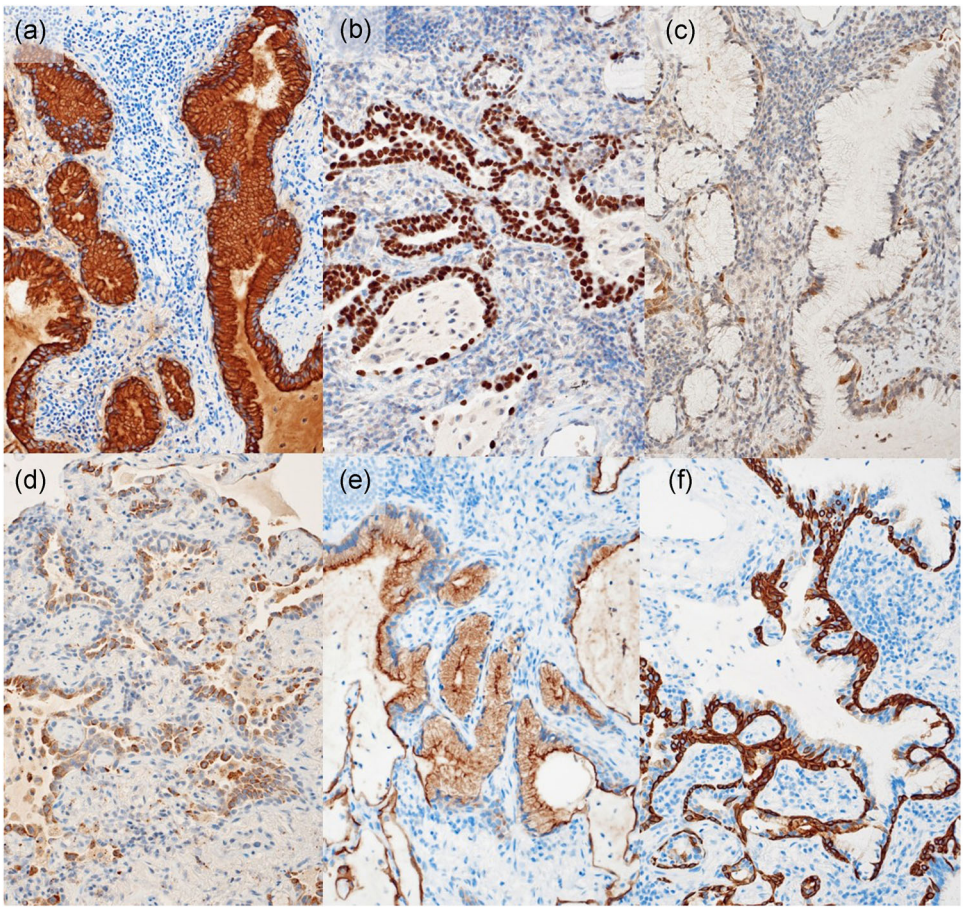

Figure 3 Immunohistochemical findings of the lung tumor. (**a**) Cytokeratin (CK)7, (**b**) Thyroid transcription factor-1 (TTF-1), (**c**) Cyclin-dependent kinase inhibitor p16 ($p16^{INK4a}$), (**d**) napsin A, (**e**) Mucin (MUC)1, and (**f**) CK5/6 (**a**–**f**: original magnification ×200). CK7 and TTF-1 are diffusely positive in both the columnar and basal cells. $p16^{INK4a}$ is partly expressed in both cell types. The columnar cells are immunoreactive for napsin A and MUC1 while the basal cells are negative. CK5/6 clearly decorates the basal cells.

deletions (10%), *EGFR* exon 20 insertions (10%), *Kirsten-RAS* mutations (24%), and *Harvey-RAS* mutations (5%), supporting a truly neoplastic process of BA.[2] In the present case, however, no gene mutations were identified.

The gene promotor methylation of tumor suppressor $p16^{INK4a}$ (often simply referred to p16) has also been detected in non-small cell lung carcinoma (NSCLC), leading to loss of expression of $p16^{INK4a}$ protein.[11] Together with the

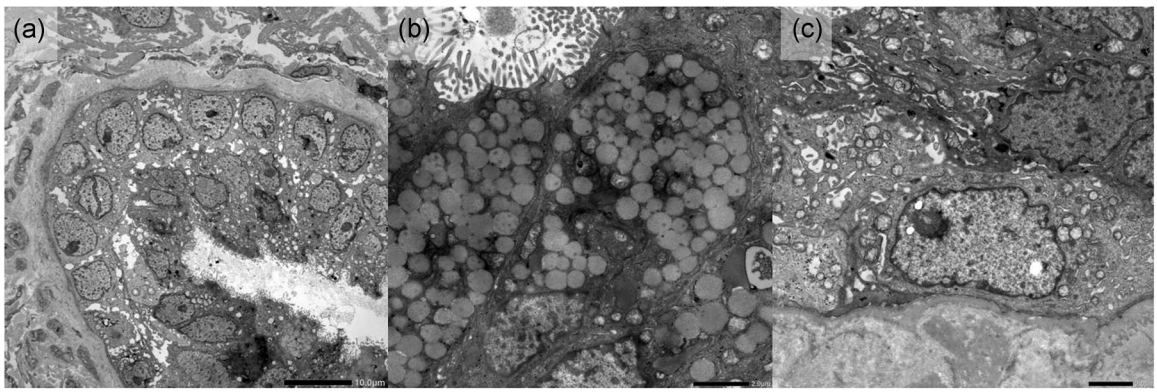

Figure 4 Electron microscopic findings of the lung tumor. (**a**) The bronchiolar epithelial tubules consist of two layers; the inner non-ciliated microvillous cells and outer basal-like cells (bar = 10 μm). (**b**) Some of the inner cells are filled with mucin granules in the cytoplasm (bar = 2 μm). (**c**) The cytoplasm of the basal cells is scanty (bar = 2 μm).

Table 1 Summary of the clinical features of previously reported BA cases and the present case

First author/Publication year	Age (years)/sex	Location	Size (mm)	CT findings	Treatment	Outcome (months)
Present case	77F	RLL	8	GGO	WR	6 NED
Ishikawa[1] 2002	50F	RUL	15	Nodule	Lobectomy	120 NED
Harada[3] 2008	62M	LLL	9	Nodule	WR	24 NED
Sato[3] 2010	67M	RUL	8	Nodule with GGO	WR	10 NED
Hata[3] 2013	59F	RLL	5	GGO with cavity	WR	18 NED
Chuang[3] 2014	68M	RLL	12	GGO	WR	48 NED
Kamata[3] 2015	61M	RUL	10	Nodule	WR	76 NED
	60F	LLL	15	Nodule	WR	33 NED
	78M	RLL	9	Nodule	Segmentectomy	66 NED
	63M	RLL	11	Nodule	Lobectomy	63 NED
	75M	LLL	6	Nodule	WR	44 NED
	62F	LLL	13	NWC	WR	45 NED
	57M	RLL	12	Nodule	WR	7 NED
	56M	RLL	11	Nodule	WR	4 NED
	66M	LLL	7	Nodule	WR	88 NED
	61F	RLL	6	Nodule	WR	2 NED
Ishikawa[3] 2016	66M	RUL	10	Nodule	Lobectomy	58 NED
	82F	LLL	10	Nodule	PR	55 NED
	77M	LLL	N/A	Nodule	Lobectomy	48 NED
	70M	RLL	30	GGO	PR	19 NED
	67F	RLL	5	Nodule	PR	28 NED
Kon[3] 2016	80M	LLL	7	Nodule	WR	29 NED
	67M	RLL	10	Nodule	WR	25 NED
	66M	RLL	13	NWC	Lobectomy	14 NED
	73F	LUL	9	NWC	WR	5 NED
	70F	RUL	8	Nodule	WR	48 NED
Lau[4] 2016	19F	RLL	13	Nodule	WR	N/A
Liu[3] 2016	60M	RLL	8	Nodule	WR	7 NED
	83F	RML	4	Nodule	Lobectomy	N/A
	81F	LL	3 to 4	Nodule	WR	N/A
	71F	LUL	12	Nodule	WR	120 NED
Chu[5] 2017	56M	LUL	11	Nodule	WR	5 NED
Jin[3] 2017	59F	RLL	8	NWC	WR	6 NED
Kim[6] 2017	73M	LLL	9	GGO	WR	36 NED
Taguchi[3] 2017	84F	RLL	8	Nodule	WR	10 NED
Udo[3] 2017	Med: 67 (M:F = 0:4)	N/A	Med: 11	N/A	Lobectomy &segmentectomy	N/A
Chang[2] 2018	Med: 72 (M:F = 11:10)	N/A	Ave: 6 (2 to 11)	Solid/GGO/ mixed	WR	Med 11: (1 to 108) NED
Kataoka[7] 2018	58F	N/A	11	N/A	Lobectomy	21 NED
	69F	N/A	4	N/A	PR	51 NED
	71M	N/A	5	N/A	PR	17 NED
	66M	N/A	6	N/A	PR	36 NED
Miyai[8] 2018	67F	RML	18	Nodule	WR	4 NED
Mikubo[9] 2019	69M	LLL	12	Nodule	WR	8 NED
Shao[3] 2019	58F	LLL	8	GGO	WR	N/A
	66F	RLL	6	Nodule	WR	N/A
Shen[10] 2019	58M	RLL	11	Nodule	WR	N/A
	64F	LLL	8.5	Nodule	WR	N/A

Abbreviations: Ave, average; GGO, ground-glass opacity; LLL, left lower lobe; LUL, left upper lobe; Med, median; N/A, not applicable; NED, no evidence of disease; NWC, nodule with cavity; PR, partial resection; RUL, right upper lobe; RML, right middle lobe; WR, wedge resection.

key tumor suppressors P14ARF and P15INK4b, $p16^{INK4a}$ is encoded by the *INK4/ARF* locus, one of the most affected genomic regions in human cancer cells.[11,12] Zhou *et al.*[12] investigated the aberrant expression of $p16^{INK4a}$ in primary NSCLC. They found that $p16^{INK4a}$ was detected in 50.7% of adenocarcinomas and 35.2% of squamous cell carcinomas. In adenocarcinoma of the lung, $p16^{INK4a}$-positive lesions accompanied a favorable clinical outcome, when compared with $p16^{INK4a}$-negative tumors. Kim *et al.*[6] reported a case of BA harboring *BRAF* V600E mutation and $p16^{INK4a}$ overexpression without evidence of HPV infection. They proposed a concept of oncogene-induced senescence (OIS). The present case also showed overexpression of $p16^{INK4a}$ unrelated to HPV infection.

BRAF V600E mutation is frequently found in various benign tumors. Most melanocytic nevi and a subset of colonic serrated polyps/adenomas show the mutation.[6] Mutation of oncogenic *BRAF* induces proliferation of melanocytes and crypt epithelial cells, leading to formation of a tumorous mass. However, most of them do not show continuous proliferation or progress to malignant tumors. Nevi and hyperplastic crypts remain dormant for a long period of time with low proliferative activity. Similarly, accelerated expression of $p16^{INK4a}$ provokes senescence-associated acidic-β-galactosidase activity, namely representing OIS.[6] Reportedly, mixed squamous cell and glandular papilloma of the lung expresses $p16^{INK4a}$.[13] In the present case, BA showed the aberrant overexpression of $p16^{INK4a}$. $p16^{INK4a}$ may function as one of the favorable prognostic markers in pulmonary glandular neoplasms.

We present for the first-time ultrastructural findings of BA. The bronchiolar epithelial tubules consisted of two layers; the inner nonciliated microvillous luminal cells and outer basal cells. Some of the luminal cells were filled with mucin granules in the cytoplasm. The cytoplasm of the basal cells was scanty. Wu *et al.*[14] reported p63 immunoreactivity in both precursor lesions and adenocarcinoma *in situ*, and the p63-positive cells belonged to atypical epithelial cells. p63 was negative in well-differentiated adenocarcinoma: namely, the malignant neoplastic lesions contained no basal cells. For the differential diagnosis of BA and malignancy, not only immunohistochemical study but also ultrastructural analysis must be useful.

The present lesion was misdiagnosed as adenocarcinoma in the intraoperative frozen section diagnosis. The frozen sections showed central glandular growth with peripheral spreading of mucin-containing columnar cells along the alveolar wall. Close observation of the permanent slides exhibited that the tumor was consistently composed of ciliated and nonciliated mucous columnar cells and basal cells. The presence of basal cells was confirmed by immunostaining for CK5/6, p40, p63 and podoplanin afterwards. Pathologists must be aware of the possibility of BA, particularly in the setting of frozen section diagnosis.

A similar benign lesion named peribronchiolar metaplasia should additionally be discussed. Peribronchiolar metaplasia represents a small airway lesion consisting of ciliate, columnar and mucinous cells often accompanying a mucin lake, and is usually associated with interstitial lung disorders. This reactive lesion typically appears as multiple fibrotic nodules around growing ciliated bronchiolar cells as a process of airway-centered (centrilobular) interstitial fibrosis.[15] The lung lesion in the present case was solitary without interstitial changes, to be distinguished from peribronchiolar metaplasia.

In conclusion, despite its rarity, BA should be considered when cytological, histological, immunohistochemical or electron microscopic evaluations of a solitary peripheral lung nodule reveal nonatypical ciliated or nonciliated mucous cells surrounded by secreted mucin. It is expected that computed tomography image analysis should accelerate the detection of a small mucinous lung lesion. Further data collection is required for clarifying the radio-clinicopathological characteristics of BA.

ACKNOWLEDGMENTS

We thank Kengo Akisawa, M.T., Special Reference Laboratories, Hachioji, and Naoki Ooishi, M.T., Department of Diagnostic Pathology, Shimada Municipal Hospital, for their skillful technical assistance. Kazuya Shiogama, M.T., Ph.D., Division of Morphology and Cell Function, Faculty of Medical Technology, Fujita Health University School of Health Sciences, kindly performed ISH for HPV detection.

DISCLOSURE STATEMENT

None declared.

AUTHOR CONTRIBUTIONS

Each author has participated sufficiently in the work to take public responsibility for appropriate portions of the content: MT and YT analyzed histopathological features and drafted the manuscript. MS, JK and TI, a team of attending doctors of the present case, earnestly discussed clinical problems. YY provided valuable advice and suggestions as a histopathologic consultant and contributed to part of the molecular study. All authors read and approved the final manuscript.

REFERENCES

1 Ishikawa Y. Ciliated muconodular papillary tumor of the peripheral lung: Benign or malignant. *Pathol Clin Med* 2002; **20**: 964–65. (*in Japanese*).

2 Chang JC, Montecalvo J, Borsu L *et al.* Bronhiolar adenoma: Expansion of the concept of ciliated muconodular papillary tumors with proposal for revised terminology based on morphologic immunophenotypic, and genomic analysis of 25 cases. *Am J Surg Pathol* 2018; **42**: 1010–26.
3 Shao K, Wang Y, Xue Q *et al.* Clinicopathological features and prognosis of ciliated muconodular papillary tumor. *J Cardiothorac Surg* 2019; **14**: 143.
4 Lau KW, Aubry MC, Tan GS, Lim CH, Takano AM. Ciliated muconodular papillary tumor: A solitary peripheral lung nodule in a teenage girl. *Hum Pathol* 2016; **49**: 22–26.
5 Chu HH, Park SY, Cha EJ. Ciliated muconodular papillary tumor of the lung: The risk of false-positive diagnosis in frozen section. *Hum Pathol: Case Rep* 2017; **7**: 8–10.
6 Kim L, Kim YS, Lee JS *et al.* Ciliated muconodular papillary tumor of the lung harboring BRAF V600E mutation and p16^{INK4a} overexpression without proliferative activity may represent an example of oncogene-induced senescence. *J Thorac Dis* 2017; **9**: E1039–44.
7 Kataoka T, Okudela K, Matsumura M *et al.* A molecular pathological study of four cases of ciliated muconodular papillary tumors of the lung. *Pathol Int* 2018; **68**: 353–58.
8 Miyai K, Takeo H, Nakayama T *et al.* Invasive form of ciliated muconodular papillary tumor of the lung: A case report and review of the literature. *Pathol Int* 2018; **68**: 530–55.
9 Mikubo M, Maruyama R, Kakinuma H, Yoshida T, Satoh Y. Ciliated muconodular papillary tumors of the lung: Cytologic features and diagnostic pitfalls in intraoperative examinations. *Diagn Cytopathol* 2019; **47**: 716–19.
10 Shen L, Lin J, Ren Z *et al.* Ciliated muconodular papillary tumor of the lung: Report of two cases and review of the literature. *J Surg Case Rep* 2019; **8**: 1–3.
11 Tuo L, Sha S, Huayu Z, Du K. *p16^{INK4a}* gene promotor methylation as a biomarker for the diagnosis of non-small cell lung cancer: An updated meta-analysis. *Thorac Cancer* 2018; **9**: 1032–40.
12 Zhou Y, Höti N, Ao M *et al.* Expression of p16 and p53 in non-small-cell lung cancer: Clinicopathological correlation and potential prognostic impact. *Bimark Med.* 2019; **13**: 761–71.
13 Miyoshi R, Menju T, Yoshizawa A, Date H. Expression of p16^{Ink4a} in mixed squamous cell and glandular papilloma of the lung. *Pathol Int* 2017; **67**: 306–10.
14 Wu M, Orta L, Gil J, Li G, Hu A, Burstein DE. Immunohistochemical detection of XIAP and p63 in adenomatous hyperplasia, atypical adenomatous hyperplasia, bronchioloalveolar carcinoma and well-differentiated adenocarcinoma. *Mod Pathol* 2008; **21**: 553–58.
15 Fukuoka J, Franks TJ, Colby TV *et al.* Peribronchiolar metaplasia: A common histologic lesion in diffuse lung disease and a rare cause of interstitial lung disease: Clinicopathologic features of 15 cases. *Am J Surg Pathol* 2005; **29**: 948–54.